Inorganica Chimica Acta, *121* (1986) 199–206

Solid State Structure and Reactivity in Solution.
8. Implications of the Structure of [1,2-Bis(diphenylphosphino)ethane]tetracarbonylmolybdenum(0) to the Chelate Effect*

IVAN BERNAL**, GEORGE M. REISNER
Department of Chemistry, University of Houston, Houston, Tex. 77004, U.S.A.
GERARD R. DOBSON** and CHARLES B. DOBSON
Department of Chemistry, North Texas State University, Denton, Tex. 76203-5068, U.S.A.

(Received May 6, 1986)

Abstract

The structure of (diphos)Mo(CO)$_4$ (diphos = 1,2-bis(diphenylphosphino)ethane) has been determined by single crystal X-ray crystallography. The crystals are orthorhombic with $a = 22.600(8)$, $b = 16.799(4)$ and $c = 14.587(4)$ Å, space group *Pbca*, $D_{\text{calc.}} = 1.45$ g cm^{-3} and $Z = 8$. The structure was solved by the Patterson technique and refined by full-matrix least-squares methods to $R = 0.044$ using 2206 reflections measured on a four-circle diffractometer. The coordination about the central molybdenum atom is a distorted octahedron, the greatest deviation from ideal geometry being the P1–Mo–P2 angle (80.2(1)°). Other distortions are induced through steric interaction between the phenyl and the carbonyl groups. The structure of (diphos)Mo(CO)$_4$ is compared to that previously reported for *cis*-(MePh$_2$P)$_2$Mo(CO)$_4$; the two molecules differ only that two methyl groups of the latter complex are replaced by the –CH$_2$CH$_2$– backbone in the former. The influence of this difference is discussed both in terms of molecular distortions induced by the presence of the chelate ring and their influence on reactivity via chelate ring-opening and -closure.

Introduction

The chelate effect, kinetically, has been discussed in terms of the less unfavorable entropy effect expected upon unimolecular chelate ring-closure than for bimolecular interaction of a unidentate ligand and a metal atom [1]. Alternatively, it has been attributed to a high 'effective concentration' of the free end of the bidentate ligand in the vicinity of the vacant coordination site [2]. Ignoring, for the moment, any other factors which may be important to the chelate effect on reactivity, such as a loss of degrees of freedom as the flexibility of the bidentate ligand is decreased upon chelation, it is anticipated that, based upon these ideas, the rate of ring-closure will be significantly greater than the rate of bimolecular interaction of a monodentate ligand with the metal.

It has been widely observed for (chelate)M(CO)$_4$ complexes (M = Cr, Mo, W) in which displacement of a chelate ring by a monodentate ligand takes place through competition between ring-closure and attack at a vacant coordination site by that monodentate ligand, that the expectation that chelate ring-closure should be faster than the bimolecular process has been borne out. For the simplest example of this process, for the mechanism (1), the steady-state rate law (assuming a steady-state concentration of the intermediate (1b)) is

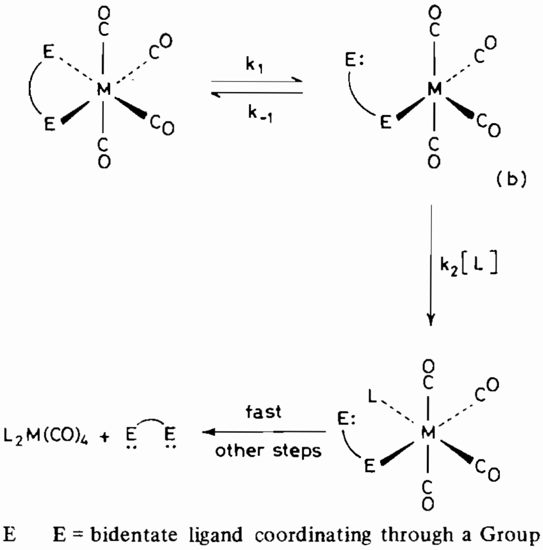

(1)

E E = bidentate ligand coordinating through a Group VA or VIA donor atom.

---

*Part 7: ref. 5.

**Authors to whom correspondence may be addressed.

0020-1693/86/$3.50

A limiting second-order rate law, expected from (2) when k_{-1} is much greater than k_2, is observed in many instances [3].

$$-d[S]/dt = k_1k_2[S][L]/(k_{-1} + k_2[L]) \qquad (2)$$

For a significant number of systems, however, the rates of chelate ring-closure, governed by k_{-1}, and of bimolecular interaction of the incoming nucleophile, L, governed by k_2, are competitive [4]. This unexpected result has been attributed to an enthalpy barrier to ring-closure which counterbalances the less unfavorable entropy of activation anticipated for the ring-closure process [3c]. In studies which involve chelate ring-opening upon pulsed laser flash photolysis, activation parameters for ring-closure *vs.* attack at the vacant coordination site by L have been obtained which support this proposal. Thus, the enthalpy of activation for chelate ring-closure in (DTN)W(CO)$_4$ in chlorobenzene (DTN = 2,2,8,8-tetramethyl-3,7-dithianonane) is 4.9(11) kcal/mol greater than that observed for bimolecular interaction of tri(isopropyl) phosphite with the ring-opened intermediate (see (1)), while, as expected, the entropy of activation for the latter process is 15.5(36) e.u. more negative for the bimolecular process [5].

In this and other systems it has been proposed that the enthalpy barrier arises as a result of distortions induced in the chelated complex upon ring-closure as a consequence, *inter alia*, of the conformational requirements of the chelating ring. In several (chelate)M(CO)$_4$ complexes, X-ray crystallographic investigations have revealed that distortions from ideal octahedral geometry do indeed exist [3d, 6].

However, this observation does not provide clear-cut evidence in support of this explanation for the enthalpy barrier resulting through chelate ring-closure, in the absence of a comparison of the structures of two complexes, similar save that one contains a chelating ring, the other two monodentate ligands. Unfortunately, such a comparison is not available for an octahedral metal carbonyl system.

The report of the crystal structure of *cis*-(MePh$_2$P)$_2$-Mo(CO)$_4$ by Cotton, Darensbourg and coworkers [7] has provided the opportunity for such a comparison, with (diphos)Mo(CO)$_4$ (diphos = 1,2-bis(diphenylphosphino)ethane; the two molecules differ only in that the two methyl groups in the former complex are replaced by a $-CH_2CH_2-$ backbone in the latter. Moreover, since, in contrast to the behavior exhibited by many other metal tetracarbonyl complexes containing chelating ligands, chelate ring displacement is not observed to take place upon reaction of (diphos)-Mo(CO)$_4$ with Lewis bases [8], the possible influence of structure on chelate ring-opening can be investigated. In this communication the structure of (diphos)Mo(CO)$_4$ is reported, together with its comparison to that of *cis*-(MePh$_2$P)$_2$Mo(CO)$_4$, so that the influences on reactivity of chelate ring-closure can be further probed.

TABLE I. Summary of Data Collection and Processing Parameters

Space group	*Pbca*
Cell constants	
a (Å)	22.600(8)
b (Å)	16.799(4)
c (Å)	14.587(4)
Cell volume *V* (Å^3)	5538.1
Molecular formula	$C_{30}H_{24}O_4P_2Mo$
Molecular weight (g mol)	606.1
Density (calc) (g cm^{-3})	1.45
Z	8
Radiation	Mo Kα (λ = 0.71073 Å)
Absorption coefficient μ (cm^{-1})	5.5
Data collection range	$4.0 \leq 2\theta \leq 42.0$
Scan width	$\Delta\theta = (1.0 + 0.35 \tan\theta)$
Maximum scan time (s)	180
Scan speed range (° min^{-1})	0.20–4.03
Total data collected	3350
Data with $I \geq 3\sigma(I)$ [a]	2206
Total variables[b]	172
$R = \Sigma\|\|F_o\| - \|F_c\|\|/\Sigma\|F_o\|$ [c]	0.044

[a]The difference between total data collected and this number is due to subtraction of standards, redundant data and reflections which do not meet the criterion of having $I \geq 3\sigma(I)$. [b]Refinement carried out with rigid body constraints on the four phenyl rings which had individual, isotropic, thermal parameters for the carbons and an overall, isotropic, thermal parameter for the five hydrogens on each ring. [c]Unit weights were used in data processing – see Refinement.

Experimental

Diphos and (diphos)Mo(CO)$_4$ were prepared by the method of Chatt and Watson [9]. The latter was slowly recrystallized from toluene/hexane at 0 °C to afford colorless, transparent plates which were found to be suitable for X-ray analysis.

A crystal of dimensions 0.4 × 0.3 × 0.1 mm was mounted on an ENRAF-NONIUS CAD-4 computer-controlled diffractometer. A summary of the crystallographically-important parameters for data collection and processing is given in Table I. Accurate cell constants determination and data collection were similar to those described elsewhere and thus are not repeated here [6a]. Two standard reflections were monitored periodically during the course of the data collection as a check of crystal stability and electronic reliability, and these did not vary significantly. In reducing the data, Lorentz and polarization factors were applied, as was an empirical absorption based on azimuthal psi scans of eight reflections having chi near 90° [10]. Data processing and calculations were made by using Molecular Structure Corporation's TEXRAY 230 modifications of the SDP-PLUS series

TABLE II. Atomic Coordinates and Thermal Parameters (×1000(×10000 for Mo))

Atom	x/a	y/b	z/c	U_{11}	U_{22}	U_{33}	U_{12}	U_{13}	U_{23}
Mo	0.11911(3)	−0.01602(3)	0.10558(4)	481(4)	359(4)	288(3)	−16(3)	−24(3)	−26(3)
P1	0.22202(9)	0.03714(11)	0.11967(14)	49(1)	46(1)	38(1)	−3(1)	3(1)	−2(1)
P2	0.11650(9)	0.03135(10)	0.26765(12)	48(1)	38(1)	32(1)	−1(1)	0(1)	−3(1)
O1	0.1313(3)	−0.0782(4)	−0.0964(4)	136(6)	88(4)	41(4)	2(4)	7(4)	−21(3)
O2	−0.0164(3)	−0.0568(3)	0.1063(4)	59(4)	67(4)	86(5)	−13(3)	−18(4)	14(3)
O3	0.0815(3)	0.1588(4)	0.0477(4)	144(6)	46(4)	64(4)	16(4)	−12(4)	15(3)
O4	0.1559(3)	−0.1863(4)	0.1802(4)	110(5)	52(4)	71(4)	18(4)	10(4)	13(3)
C1	0.1268(4)	−0.0544(4)	−0.0236(6)	83(7)	48(5)	38(5)	−2(5)	2(5)	−4(4)
C2	0.0342(4)	−0.0438(4)	0.1054(5)	71(6)	36(4)	39(5)	0(4)	−13(5)	3(4)
C3	0.0952(4)	0.0967(5)	0.0656(5)	69(6)	55(6)	33(4)	−3(5)	−2(4)	−4(4)
C4	0.1431(4)	−0.1250(5)	0.1529(5)	70(6)	49(5)	36(4)	0(4)	4(4)	−5(4)
C5	0.2255(4)	0.0968(5)	0.2258(5)	47(5)	60(5)	46(5)	−12(4)	3(4)	−11(4)
C6	0.1930(3)	0.0539(5)	0.3030(5)	52(5)	63(5)	35(4)	−3(4)	−1(4)	−8(4)
C7	0.2509(2)	0.1067(3)	0.0326(3)	46(2)					
C8	0.2229(2)	0.1106(3)	−0.0525(3)	64(2)					
C9	0.2430(2)	0.1639(3)	−0.1189(3)	72(3)					
C10	0.2912(2)	0.2133(3)	−0.1001(3)	71(3)					
C11	0.3192(2)	0.2093(3)	−0.0150(3)	70(3)					
C12	0.2990(2)	0.1560(3)	0.0513(3)	64(2)					
C13	0.2817(2)	−0.0373(3)	0.1315(3)	44(2)					
C14	0.3285(2)	−0.0298(3)	0.1933(3)	65(2)					
C15	0.3712(2)	−0.0894(3)	0.1992(3)	82(3)					
C16	0.3672(2)	−0.1566(3)	0.1434(3)	81(3)					
C17	0.3204(2)	−0.1641(3)	0.0816(3)	70(3)					
C18	0.2776(2)	−0.1045(3)	0.0757(3)	56(2)					
C19	0.0871(2)	−0.0303(3)	0.3602(3)	39(2)					
C20	0.0919(2)	−0.0061(3)	0.4514(3)	56(2)					
C21	0.0655(2)	−0.0511(3)	0.5206(3)	67(2)					
C22	0.0342(2)	−0.1201(3)	0.4987(3)	66(2)					
C23	0.0294(2)	−0.1442(3)	0.4074(3)	64(2)					
C24	0.0558(2)	−0.0993(3)	0.3382(3)	55(2)					
C25	0.0740(2)	0.1228(2)	0.2861(3)	44(2)					
C26	0.0155(2)	0.1229(2)	0.2553(3)	56(2)					
C27	−0.0203(2)	0.1892(2)	0.2704(3)	71(3)					
C28	0.0023(2)	0.2555(2)	0.3162(3)	73(3)					
C29	0.0607(2)	0.2554(2)	0.3470(3)	70(2)					
C30	0.0966(2)	0.1891(2)	0.3319(3)	60(2)					
H51	0.2060(3)	0.1494(5)	0.2148(5)	47(14)					
H52	0.2677(3)	0.1054(5)	0.2435(5)	47(14)					
H61	0.2143(3)	0.0031(5)	0.3173(5)	65(17)					
H62	0.1922(3)	0.0884(5)	0.3588(5)	65(17)					
H8	0.1884(2)	0.0753(3)	−0.0660(3)	161(18)					
H9	0.2230(2)	0.1668(3)	−0.1799(3)	161(18)					
H10	0.3056(2)	0.2515(3)	−0.1477(3)	161(18)					
H11	0.3537(2)	0.2447(3)	−0.0016(3)	161(18)					
H12	0.3191(2)	0.1532(3)	0.1123(3)	161(18)					
H14	0.3314(2)	0.0184(3)	0.2333(3)	119(14)					
H15	0.4048(2)	−0.0840(3)	0.2435(3)	119(14)					
H16	0.3978(2)	−0.1994(3)	0.1476(3)	119(14)					
H17	0.3175(2)	−0.2123(3)	0.0416(3)	119(14)					
H18	0.2441(2)	−0.1099(3)	0.0314(3)	119(23)					
H20	0.1143(2)	0.0433(3)	0.4672(3)	203(23)					
H21	0.0689(2)	−0.0338(3)	0.5860(3)	203(23)					
H22	0.0153(2)	−0.1523(3)	0.5483(3)	203(23)					
H23	0.0070(2)	−0.1937(3)	0.3917(3)	203(23)					
H24	0.0524(2)	−0.1165(3)	0.2728(3)	203(23)					
H26	−0.0007(2)	0.0754(2)	0.2225(3)	130(15)					
H27	−0.0622(2)	0.1892(2)	0.2483(3)	130(15)					
H28	−0.0235(2)	0.3030(2)	0.3270(3)	130(15)					
H29	0.0769(2)	0.3029(2)	0.3798(3)	130(15)					
H30	0.1385(2)	0.1891(2)	0.3540(3)	130(15)					

of programs. The structure was solved by the Patterson technique which revealed the position of the Mo atom. All the remaining non-hydrogen atoms were found from successive difference Fourier maps. Since there was no reason to expect any distortions in the four phenyl rings, these were refined as rigid

TABLE III. Molecular Geometry with Estimated Standard Deviations in Parentheses

(a) Bond lengths (Å)

Mo–P1	2.500(2)	P2–C6	1.844(8)
Mo–P2	2.495(2)	P2–C19	1.827(4)
Mo–C1	1.999(8)	P2–C25	1.832(4)
Mo–C2	1.974(8)	C1–O1	1.140(8)
Mo–C3	2.053(9)	C2–O2	1.164(9)
Mo–C4	2.030(9)	C3–O3	1.120(9)
P1–C5	1.846(7)	C4–O4	1.143(9)
P1–C7	1.845(4)	C5–C6	1.525(10)
P1–C13	1.847(4)		

(b) Bond angles (°)

P1–Mo–P2	80.2(1)	Mo–P2–C6	108.0(2)
P1–Mo–C1	96.4(3)	Mo–P2–C19	121.9(2)
P1–Mo–C2	171.4(2)	Mo–P2–C25	114.8(2)
P1–Mo–C3	86.5(2)	C6–P2–C19	104.5(3)
P1–Mo–C4	92.6(2)	C6–P2–C25	106.2(3)
P2–Mo–C1	176.3(3)	C19–P2–C25	100.1(2)
P2–Mo–C2	93.1(2)	P1–C5–C6	110.0(5)
P2–Mo–C3	88.2(2)	P2–C6–C5	110.0(5)
P2–Mo–C4	88.4(2)	P1–C7–C8	118.8(2)
C1–Mo–C2	90.4(3)	P1–C7–P12	121.1(2)
C1–Mo–C3	93.0(3)	P1–C13–C14	123.5(2)
C1–Mo–C4	90.4(3)	P1–C13–C18	116.4(2)
C2–Mo–C3	87.8(3)	P2–C19–C20	120.8(2)
C2–Mo–C4	92.7(3)	P2–C19–C24	119.0(2)
C3–Mo–C4	176.6(3)	P2–C25–C26	116.7(2)
Mo–P1–C5	107.6(3)	P2–C25–C30	123.3(2)
Mo–P1–C7	111.9(2)	Mo–C1–O1	178.3(7)
Mo–P1–C13	116.4(2)	Mo–C2–O2	177.0(7)
C5–P1–C7	102.6(3)	Mo–C3–O3	176.9(7)
C5–P1–C13	105.0(3)	Mo–C4–O4	179.0(7)
C7–P1–C13	103.6(2)		

bodies with idealized hydrogens. Since these calculations could not be carried out using the TEXRAY 230 programs, further refinement was performed using the SHELX 76 series of programs [11].

Isotropic refinement of all the non-hydrogens converged to $R = 0.079$. Anisotropic refinement of all non-hydrogens except the carbons of the phenyl rings (which were refined as rigid bodies having C–C bonds of 1.395 Å and idealized hydrogens at C–H = 1.00 Å) and isotropic refinement of the hydrogens converged at $R = 0.044$*. The estimated standard deviations were computed from the inverse matrix of the final full-matrix least-squares cycle. No unusually high correlations were noted among any variables in the final cycle. Final atomic coordinates and thermal parameters are presented in Table II. Interatomic distances and angles are given in Table III. For other data see 'Supplementary Material'. The stereo drawings (Figs. 1 and 2) were obtained through use of Johnson's ORTEP [12].

Results and Discussion

The Structure of (Diphos)Mo(CO)$_4$

The molecule consists of a central Mo atom bonded to four carbonyls and a bidentate ligand having two phosphorus atoms as donors. The coordination around the metal is a distorted octahedron, the equatorial plane being formed by two carbonyl groups (C1 and C2) and the two phosphorus atoms. The deviation of the Mo atom from this plane is 0.04 Å. Distortions from the theoretical octahedral geometry are largely due to the formation of the five-membered chelate ring and also to the differences between the Mo–P and Mo–carbonyl bond lengths. The two Mo–P distances are virtually identical (2.500(2) and 2.495(2) Å), which is expected since the environments about the two phosphorus atoms are similar. Moreover, they fall within the range of Mo–P distances previously reported for other molybdenum tetracarbonyl complexes [7, 13] and are

---

*Throughout the last cycle of least squares refinement unit weights were employed since a weighted refinement ($w = 1/[\sigma^2(F_o)]$) gave poorer results in terms of the R factor, the geometry of the molecule, and e.s.d. values.

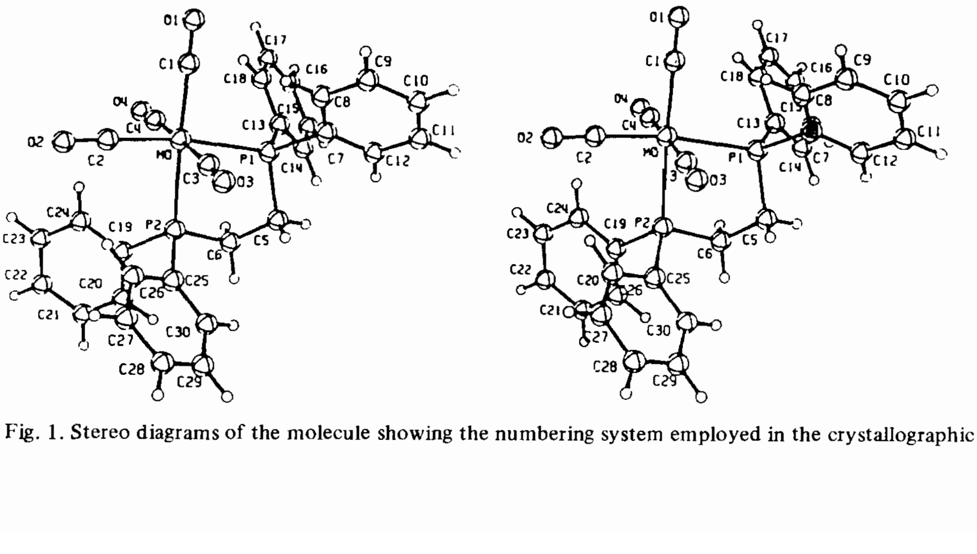

Fig. 1. Stereo diagrams of the molecule showing the numbering system employed in the crystallographic study.

significantly shorter than 2.71 Å, the sum of the covalent radii (1.61 Å for molybdenum and 1.10 Å for phosphorus) [14]. This shortening is ascribed largely to d_π–d_π back-donation from molybdenum to phosphorus.

In this structure the four Mo-carbonyl distances (1.999(8), 1.974(9), 2.053(9) and 2.030(9) Å) fall into two distinct groups whose mean values are 1.986 and 2.041 Å. The two mutually *trans* carbonyl groups have longer Mo–C distances than do the two carbonyls each *trans* to the phosphorus atoms. These trends are expected since P is known to be a poorer π-acceptor than CO, and on the basis of the directional nature of π-bonding in substituted octahedral metal carbonyls [15].

The differences among the four carbon-oxygen bond lengths are small, although the trend observed is that expected on the basis of the complementary nature of the Mo–C and C–O bonds. The carbonyl groups are coordinated to the metal atom in the usual angular fashion. All four M–C–O angles are slightly less than 180°, the deviation from linearity being largest for C3–O3 (176.9(7)°).

A large deviation from ideal octahedral geometry is observed for the P1–Mo–P2 angle, for which a contraction from 90° to 80.2(1)° occurs. Similar angles have been noted in related complexes containing a central molybdenum atom bonded to a bidentate ligand via two phosphorus atoms and forming a five-membered chelate ring. Thus, values of 79.7(3), 79.49(2), 79.81(7) and 79.75(7) and 79.5(2)° have been reported [13b, c, g, h]. This contraction of the P–Mo–P angle is compensated for in the equatorial plane by an increase in both P–Mo–C(*cis*) angles. The opening of the two angles, however, is not symmetrical, the P1–Mo–C1 angle being significantly larger (96.4(3)°) than is the P2–Mo–C2 angle (93.1(2)°). The C1–Mo–C2 angle remains close to 90° (90.4(3)°). It has been suggested that these asymmetric deviations are the result of steric hindrance between the carbonyl groups and the substituents on donor atoms attached to the metal [3d, 6b]. In the present case, the shortest intramolecular contact between carbonyls and the phenyl substituents is that between C1 and H8 (2.66(1) Å); no short intermolecular distances were observed. For carbonyl C2 the shortest intramolecular contact is significantly longer (C2–H26 = 2.75(1) Å). No similar short distances were observed for the two mutually *trans* carbonyls. Thus there is some steric interaction between the C1 carbon and one of the phenyls attached to P1. This strain is partially released through the somewhat larger opening of the P1–Mo–C1 angle (96.4(3)°) than the P2–Mo–C2 angle (93.1(2)°). A similar situation is noted in (DTO)W(CO)$_4$ (DTO = 2,2,7,7-tetramethyl-3,6-dithiaoctane), in which the two S–W–C(*cis*) angles are 98.0(5) and 92.6(6)°, and in (DTN)W(CO)$_4$ (DTN = 2,2,8,8-tetramethyl-3,7-dithianonane) (99.4(8) and 91.2(9)°) [6a]. The slight asymmetric opening of the two P–Mo–C(*cis*) angles observed in the present case represents an intermediate situation between symmetric deviations such as are observed for (NP)Mo(CO)$_4$ (NP = 1-diethylamino-2-(diphenylphosphino)ethane), where the two relevant angles are 96.9(2) and 96.6(3)° [6c] and the asymmetric distortions found in (DTO)Cr(CO)$_4$, in which the S–Cr–C(*cis*) angles are 99.3(1) and 90.7(2)° [6b].

The principal axes in (diphos)Mo(CO)$_4$ (P1–Mo–C2 = 171.4(2), P2–Mo–C1 = 176.3(3) and C3–Mo–C4 = 176.6(3)° also differ significantly from linearity.

The five-membered chelate ring has the expected puckered conformation, with atoms C5 and C6 above and below the plane defined by Mo, P1 and P2. The puckering is nearly symmetrical, C5 being 0.395 Å above the plane and C6 0.369 Å below it. The dihedral angle between the equatorial plane and that formed by the Mo, P1 and P2 atoms is 2.43°. Bond lengths within the chelate ring agree well with those found in the literature.

NMR Spectra of (Diphos)Mo(CO)$_4$

The 300 MHz proton NMR spectrum of (diphos)Mo(CO)$_4$ in CDCl$_3$ is shown in Fig. 3. It consists of a multiplet centered at 7.61 ppm, a singlet at 7.38 ppm, and a doublet centered at 2.55 ppm (*p*-dioxane

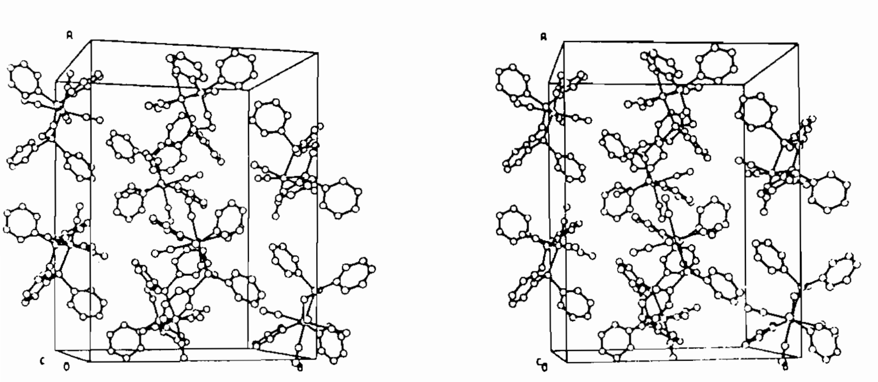

Fig. 2. Packing diagram for the molecules.

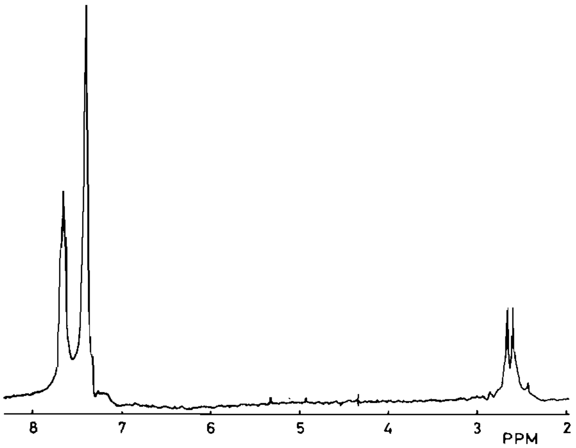

Fig. 3. Proton NMR spectrum of the (diphos)Mo(CO)$_4$ in CDCl$_3$ (*p*-dioxane as internal standard) taken at room temperature employing a 300 MHz Nicolet NT-300 WB spectrometer.

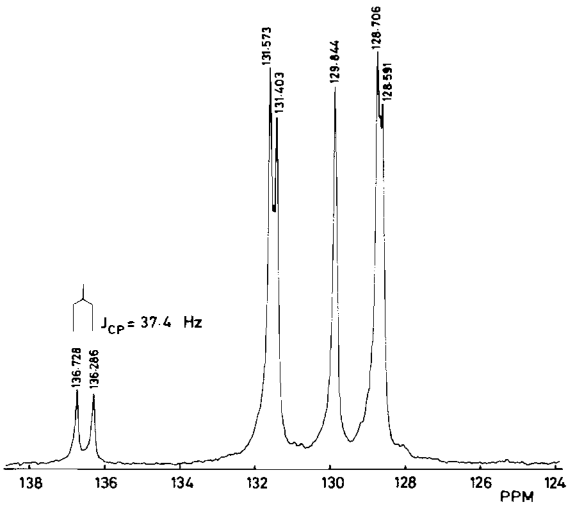

Fig. 4. ^{13}C NMR spectrum of (diphos)Mo(CO)$_4$ (CDCl$_3$ internal standard) showing the region for the aromatic carbons.

internal standard). Integration (the two peaks of the doublet were integrated together) affords a 2:3:1 ratio for the respective multiplets. The multiplet at 7.61 ppm was assigned to the eight *ortho* protons of the four phenyls, the 7.38 ppm peak to the twelve *meta* and *para* protons of the phenyls (an unresolved multiplet), and the doublet to the four ethylene protons. Thus this spectrum indicates that the four phenyls are equivalent and probably freely rotating. The carbon-13 NMR spectrum in CDCl$_3$ (Fig. 4) is consistent with this assumption. The aromatic carbon region shows three doublets and a sharp singlet, centered at 136.507, 131.488, 129.844 and 128.648 ppm (CDCl$_3$ internal standard), which were assigned to the *ipso*, *ortho*, *para* and *meta* carbons, respectively. The *ipso*, *ortho* and *meta* carbons were each ^{31}P-coupled (37.4, 12.8 and 8.7 Hz, respectively).

Comparison of the Structure of (Diphos)Mo(CO)$_4$ to Those of Related Complexes Containing Monodentate Ligands

The distortions from octahedral geometry observed in (diphos)Mo(CO)$_4$ differ from those observed in the related *cis*-L$_2$Mo(CO)$_4$ complexes (L = PMe$_2$Ph, PMePh$_2$ and PPh$_3$) [7]. In the latter complexes the means through which steric interactions are minimized are not restricted by the formation of a five-membered chelate ring. Thus, in contrast to the *ca.* 10° decrease in the P1–Mo–P2 angle from that expected for idealized octahedral geometry observed in (diphos)Mo(CO)$_4$, expansions of the P–Mo–P angles and significant increases in the P–Mo bond lengths are observed in these complexes. For example, an enormous increase in the P–Mo–P angle, to 104.62(7)°, is observed in the PPh$_3$ complex, and progressive lengthening of the average Mo–P bonds, from 2.525(3) to 2.545(1) and 2.576(2) Å along the series of complexes for L = PMe$_2$Ph, PMePh$_2$ and PPh$_3$, respectively, is also noted.

In comparing the two most closely-related complexes, (diphos)Mo(CO)$_4$ (**A**) and *cis*-(MePh$_2$P)$_2$Mo(CO)$_4$ (**B**), a significant decrease in the P1–Mo–P2 angle, from 92.52(5)° to 80.2(1)° is noted from **B** to **A** as a consequence of chelate ring formation in **A**. Also as a consequence of the presence of a ring-backbone in **A**, the relative position of the phenyl and carbonyl groups is such as to lead to intramolecular strain (Fig. 1). However, this orientation of the phenyl groups does not persist in solution at ambient temperature as indicated by the NMR spectra. In the crystal, however, this orientation produces in the molecule the short intramolecular contacts between a pair of phenyls and the equatorial carbons C1 and C2 which have been noted above with the consequent distortion of the P1–Mo–C1 and P2–Mo–C2 angles which differ significantly from those in **B**. Distortions occur also in the angles about the phosphorus. The Mo–P1–C13 and Mo–P2–C25 angles are abnormally large averaging 115.6°, while the angles and C7–P1–C13 and C25–P2–C19 are abnormally small averaging 101.9°.

The P–Mo bond lengths in the two complexes differ markedly, averaging 2.498(2) Å in **A** and 2.555(1) Å in **B**. In the series of compounds *cis*-(Me$_x$Ph$_{3-x}$)Mo(CO)$_4$ (x = 0–2) the monotonic increase in the average Mo–P bond length with an increasing value of x, noted above, was attributed to the increasing bulk of the coordinating phosphines [7]; the short Mo–P bond length noted here is consistent with the interpretation in that in **A** the conformational demands of the chelate ring produce shorter Mo–P bond lengths.

Reactivity via Ring-opening and Ring-closure

It is observed that *cis*-disubstituted tetracarbonylmolybdenum complexes containing monodentate

TABLE IV. Carbonyl Stretching Frequencies, Mo–P Bond Lengths and Reactivities via Dissociation of Mo–P Bonds for Various *cis*-$L_2Mo(CO)_4$ Complexes

L_2	ν(CO) (cm^{-1})	Average M–L bond length (Å)	Reactivity for M–L bond dissociation (k_1, s^{-1})
$(Me_2PhP)_2$	[a]2018, 1920, 1900, 1891	[c]2.529	[e]$<1 \times 10^{-6}$
$(MePh_2P)_2$	[a]2020, 1925, 1902, 1891	[c]2.555	[e]1.33×10^{-6}
$(Ph_3P)_2$	[a]2023, 1927, 1908, 1897	[c]2.572	[e]3.16×10^{-3}
$Ph_2PC_2H_4PPh_2$	[b]2020, 1925, 1912, 1894	[d]2.498	[f]0

[a]Ref. 20, C_2Cl_4 solvent. [b]Ref. 19, CS_2 solvent. [c]Ref. 7. [d]This work. [e]Ref. 7, C_2Cl_4 solvent at 70 °C. [f]Ref. 8, mesitylene solvent at 135 °C.

ligands coordinating through phosphorus undergo ligand-exchange via Mo–P bond fission, whereas (diphos)Mo(CO)$_4$ reacts via CO loss under much more drastic conditions (135 °C *vs.* 70 °C, Table IV), with no evidence for Mo–P bond fission, since no reaction products not containing diphos are noted [8]. Rates of chelate ring-opening are usually observed to be slower than the rates of monodentate ligand dissociation, an observation attributed to energetically-favored linear displacement of the ligand upon bond breaking, a pathway not available for chelating rings, for which an angular displacement is required [16]. Aside from such effects, it is instructive to consider possible influences on reactivity of the structural differences noted in (diphos)Mo(CO)$_4$ and *cis*-L_2Mo-(CO)$_4$ complexes. It is important to note that there is much evidence which suggests that the transition state leading to ring-closure (or ring-opening) is very similar in structure to that of the five-coordinate 'ring-opened' intermediate, that is, that there is much bond-breaking which takes place in attaining the transition state via ring-opening, but little bond-making which takes place upon attaining the transition state via ring-closure [17]. Therefore, influence on reactivity of structural differences in **A** and **B** should be much more pronounced for the bond-breaking process [18]. It first should be noted that the abnormally short Mo–P bond lengths in **A** are not indicative of increased d_π–d_π bonding if the criterion that such changes should be reflected in the carbonyl stretching frequencies for the complexes is applied [19]. Nor are the changes in Mo–P bond lengths observed in the series of complexes of Cotton, Darensbourg and coworkers (Table IV) explicable on this basis [7, 20]. Although the potential influence of ligand basicity on Mo–L bond lengths was noted by Cotton *et al.*, the trend in increased reactivity via Mo–P bond fission (Table IV) indeed follows the order of increasing Mo–L bond lengths in the series of *cis*-$(Me_xPh_{3-x}P)_2Mo(CO)_4$ complexes; the Table also demonstrates that (diphos)Mo(CO)$_4$ maintains the correlation between ease of Mo–P bond-breaking and Mo–P bond length. It thus would appear that sterically-induced [7, *vide supra*] changes in Mo–P bond lengths in these complexes largely influence the extent of M–P σ-bonding and that these bonding changes exert a dominant influence on the ease of Mo–P bond-breaking.

The influences which the structural differences induced by chelate ring-formation in (diphos)Mo-(CO)$_4$ would have on the activation barriers to ring-reclosure, (which, one might assume, would be similar to those which would be important in complexes which have been observed to undergo chelate ring-closure, e.g., those cited in refs. 4 and 5) are more difficult to assess. While data indicate that in this transition state there is relatively little M–P bond-making, it is clear that reorientation of the free end of the bidentate ligand will have to take place. In contrast, the two $MePh_2P$ ligands in **B**, while occupying greater space in the coordination sphere, are able more readily to undergo reorientation when entering the coordination sphere of the metal atom. Some of the angular distortions which arise as a consequence of the steric requirements of both the chelate ring and the phenyl groups in **A** may be taking place in the transition state. However, given that the structure of (diphos)Mo(CO)$_4$ probably does not closely resemble the transition state leading to ring-reclosure and thus that distortions observed in the complex may not be indicative of important influences on the energetics of this reaction pathway, it is also reasonable to conclude that restrictions imposed by the bidentate ligand on the availability of the lowest energy reaction coordinate for interaction of P with the vacant coordination site on Mo [16] also exert a significant influence on the observed enthalpy of activation.

Supplementary Material

Compilations of observed and calculated structure factors (13 pages) and least-squares planes (Table 1, one page) are available.

Acknowledgements

The support of this research by the Robert A. Welch Foundation under Grants B-434 and E-594 is gratefully acknowledged. We thank the U.S. National Science Foundation for providing funds for the purchase of the diffractometer, and the Computing Center of the University of Houston for free computing time. Drs. G. Martin and M. G. Richmond provided expert assistance with the interpretation of the NMR spectra.

References

1 F. Basolo and R. G. Pearson, 'Mechanisms of Inorganic Reactions', 2nd edn., Wiley, New York, 1967, p. 223–225.

2 G. Schwarzenbach, *Helv. Chim. Acta, 35,* 2344 (1952).

3 (a) G. C. Faber and G. R. Dobson, *Inorg. Chem., 7,* 584 (1968); (b) G. R. Dobson and Honors, Science 102-2, Spring Semester, 1977, *J. Coord. Chem., 7,* 253 (1978); (c) G. R. Dobson, Z. Y. Al-Saigh and N. S. Binzet, *J. Coord. Chem., 11,* 159 (1981); (d) D. E. Halverson, G. M. Reisner, G. R. Dobson, I. Bernal and T. L. Mulcahy, *Inorg. Chem., 21,* 4285 (1982); (e) G. R. Dobson, C. S. Binzet and J. E. Cortes, *J. Coord. Chem.,* in press.

4 (a) G. C. Faber, T. D. Walsh and G. R. Dobson, *J. Am. Chem. Soc., 90,* 4178 (1968); (b) G. R. Dobson, *Inorg. Chem., 8,* 90 (1969); (c) G. R. Dobson and G. C. Faber, *Inorg. Chim. Acta, 4,* 87 (1970); (d) W. J. Knebel and R. J. Angelici, *Inorg. Chem., 13,* 632 (1974); (e) L. D. Schultz and G. R. Dobson, *J. Coord. Chem., 5,* 163 (1976); (f) L. D. Schultz and G. R. Dobson, *J. Organomet. Chem., 124,* 19 (1976); (g) G. R. Dobson and L. D. Schultz, *J. Organomet. Chem., 131,* 285 (1977); (h) G. R. Dobson and A. Moradi-Araghi, *Inorg. Chim. Acta, 31,* 263 (1978).

5 G. R. Dobson, C. B. Dobson and S. E. Mansour, *Inorg. Chem., 24,* 2179 (1985).

6 (a) G. M. Reisner, I. Bernal and G. R. Dobson, *J. Organomet. Chem., 157,* 23 (1978); (b) G. M. Reisner, I. Bernal and G. R. Dobson, *Inorg. Chim. Acta, 50,* 227 (1981); (c) G. R. Dobson, I. Bernal, G. M. Reisner, C. B. Dobson and S. E. Mansour, *J. Am. Chem. Soc., 107,* 525 (1985).

7 F. A. Cotton, D. J. Darensbourg, S. Klein and B. W. S. Kolthammer, *Inorg. Chem., 21,* 294 (1982).

8 G. C. Faber and G. R. Dobson, *Inorg. Chim. Acta, 2,* 479 (1968).

9 J. Chatt and H. R. Watson, *J. Chem. Soc.,* 4980 (1961).

10 A. C. T. North, D. C. Phillips and F. S. Matthews, *Acta Crystallogr., Sect. A, 24,* 351 (1968).

11 G. M. Sheldrick, 'SHELX-76', program for crystal structure determination, Cambridge, U.K., 1976.

12 C. K. Johnson, 'ORTEP 2', a Fortran ellipsoid plot program for crystal structure illustrations, ORNL-5138, Oak Ridge, Tenn., 1972.

13 (a) K. K. Cheung, T. F. Lai and K. S. Mok, *J. Chem. Soc. A,* 1644 (1971); (b) F. W. B. Einstein and J. S. Field, *J. Chem. Soc., Dalton Trans.,* 1628 (1975); (c) T. Uchida, Y. Uchida, M. Hidai and T. Kodama, *Acta Crystallogr., Sect. B, 31,* 1197 (1975); (d) W. S. Sheldrick, *Acta Crystallogr., Sect. B, 32,* 308 (1976); (e) M. Hidai, T. Kodama, M. Sato, M. Harakawa and Y. Uchida, *Inorg. Chem., 15,* 2694 (1976); (f) W. S. Sheldrick and A. Barkenstein, *Acta Crystallogr., Sect. B, 33,* 2916 (1977); (g) M. Sato, T. Tatsumi, T. Kodama, M. Hidai, T. Uchida and Y. Uchida, *J. Am. Chem. Soc., 100,* 4447 (1978); (h) M. W. Bishop, J. Chatt, J. R. Dilworth, M. B. Hursthouse and M. Motevalli, *J. Chem. Soc., Dalton Trans.,* 1603 (1979); (i) M. Field, W. Handke and W. S. Sheldrick, *Z. Naturforsch., 35b,* 838 (1980); (j) G. Baccolini, L. Busetto and E. Foresti, *J. Chem. Soc., Dalton Trans.,* 1544 (1981); (k) F. A. Cotton, D. J. Darensbourg and W. H. Isley, *Inorg. Chem., 20,* 579 (1981).

14 L. Pauling, 'The Nature of the Chemical Bond', 3rd edn., Cornell University Press, Ithaca, New York, 1960.

15 F. A. Cotton and C. S. Kraihanzel, *J. Am. Chem. Soc., 84,* 4432 (1962).

16 D. W. Margerum, in 'Mechanisms of Inorganic Reactions', *Advances in Chemistry Series, 49,* 75 (1965).

17 W. A. Covey and T. L. Brown, *Inorg. Chem., 12,* 2820 (1972).

18 G. S. Hammond, *J. Am. Chem. Soc., 77,* 334 (1955).

19 R. T. Jernigan, R. A. Brown and G. R. Dobson, *J. Coord. Chem., 2,* 47 (1972).

20 D. J. Darensbourg and R. L. Kump, *Inorg. Chem., 17,* 2680 (1978).